11th ANKARA INTERNATIONAL AEROSPACE CONFERENCE **AIAC-2021-046**
8-10 September 2021 - METU, Ankara TURKEY

DEVELOPMENT OF LINEARIZED EULER SOLVERS ON FREQUENCY DOMAIN FOR OSCILLATING AIRFOILS

Ata Tankut Ardıç* and Arash Karshenass† and
Ozgur Ugras Baran‡ and Ender Cigeroglu§
Middle East Technical University
Ankara, Turkey

ABSTRACT

In this study, we present the results of our new harmonic flow solver for the solution of flow field and force response of the oscillating aerodynamic bodies. The new Linearized Euler harmonic solver relies on a new formulation based on the Flux Vector Splitting approach. This solver is very capable of solving high-speed compressible flows and validated for internal flows with pressure fluctuations. The extension of the method for compressible external flows around aerodynamic bodies can be applied for the solution of the flows around the oscillating aerodynamic bodies. For this purpose, we have extended our solver to involve such flows around oscillating arbitrary aerodynamic bodies. Necessary developments and the boundary condition implementations such as far-field and oscillating wall boundary conditions are developed and presented. These new developments allow the solution of the flow around aerodynamic bodies that are oscillate with the single prescribed perturbation with a harmonic character. Due to linearization assumptions, the input excitation frequency of the airfoil is utilized as the fluctuating frequency of whole harmonic variables in the domain. The main objective is to determine the unsteady aerodynamic forces on the tested 2D airfoil profile with prescribed motion. Airfoil validation cases are evaluated with an unsteady solver with a moving mesh and a new harmonic solver with a fixed grid. The results match well with some minor deviations, and our solver demands much less computational power.

*Research Assistant, Department of Mechanical Engineering, Email: ardic@metu.edu.tr
†PhD Candidate, Department of Mechanical Engineering, Email: aras.saygin@metu.edu.tr
‡Assistant Professor, Department of Mechanical Engineering, Email: ubaran@metu.edu.tr
§Professor, Department of Mechanical Engineering, Email: ender@metu.edu.tr

INTRODUCTION

As the popularity of CFD increases and CPU speeds fail the keep up to the demand, faster approaches than conventional time-accurate unsteady flow analysis become a necessity. For temporally periodic flows, harmonic approaches are proven to be suitable alternative with lower computational cost compared to time-domain methods. Another considerable advantage of harmonic methods is the usability of a fixed grid in space when fluid-structure interactions are scrutinized. Even for 3D systems with complicated geometries, only the mode shapes of the structure to be analyzed are sufficient if the structure motion is enforced [Howison et al., 2017].

The harmonic methods can be employed in some important external aerodynamics problems. The fluid-structure interaction problems are one of them. Especially flutter problems are extremely difficult to solve with conventional CFD methods. The structural response is often harmonic, and harmonic methods can significantly improve the solution time. Similarly, harmonic methods can be employed to calculate damping derivatives. The time-marching CFD methodology often involve prescribed harmonic motion divided into smaller time steps.

There are a few different harmonic methodologies. The linearized harmonic method, also called the Linearized Harmonic (LH) method, is the simplest among all, and it is utilized in this study. The method is firstly adapted to Euler equations by Hall [Hall, 1987], and it splits the solution into the mean and harmonic perturbation parts, assuming the mean solution is equivalent to the steady-state. There are other methods that allow the nonlinear interaction between the mean solution and the harmonic perturbation (harmonic balance, time-spectral method, and others) [Gong and Zhang, 2019; Ekici and Hall, 2011]. However, due to this non-linearity, one gets evenly spaced sub time level solutions whereas LH provides the solution at any instant within the period with some post-processing. The downside of the the LH is that perturbations cannot be captured as accurately as some other harmonic methodologies such as harmonic balance method due to the linear assumption.

On the other hand, in the Fluid-Structure Interaction (FSI) problems with single excitation frequency and low vibration amplitudes, the LH method is very advantageous. Dufour et al. demonstrated this fact in their test case study by analyzing NACA64A006 airfoil with the linearized harmonic method, unsteady CFD and commonly accepted harmonic balance methodology [Dufour et al., 2010]. In their study the solution is closed with RANS modeling in all methods. For the subsonic case, linearized methods gave the same solution as harmonic balance methodology with better efficiency. Considering the amount of computation power, linearized methods are more efficient than harmonic methods for these conditions without compromising much accuracy.

METHOD

Derivation of Linearized Euler harmonic equations starts with an integral form of unsteady inviscid equations in the normal-tangential coordinate system:

$$\frac{\partial}{\partial t}\int_{\Omega}\mathbf{W}d\Omega = -\int_{A}\mathbf{F}dA \tag{1}$$

Later, the conservative variables are decomposed into mean,$\overline{\mathbf{W}}(x,y,z)$, which is assumed to be the steady-state solution in the case of LH and harmonically fluctuating (perturbed) parts,$\widetilde{\mathbf{W}}(x,y,z,t)$ with predefined frequency ω.

$$\mathbf{W} = \overline{\mathbf{W}} + \widetilde{\mathbf{W}} \tag{2}$$

so that (1) is rewritten as following

$$\frac{\partial}{\partial t}\int_{\Omega}(\overline{\mathbf{W}} + \widetilde{\mathbf{W}})d\Omega = -\int_{A}\mathbf{F}dA \tag{3}$$

Another assumption is that unsteady convective fluxes can also be decomposed into steady-state and perturbation components similar to conservative variables. Applying Taylor series over $\mathbf{F}$ around $\overline{\mathbf{W}}$yields to

$$\mathbf{F} \approx \overline{\mathbf{F}} + \left.\frac{\partial \mathbf{F}}{\partial \mathbf{W}}\right|_{\overline{W}}(\mathbf{W}-\overline{\mathbf{W}}) + O^2(\mathbf{W}-\overline{\mathbf{W}}) + ... = \overline{\mathbf{F}} + [\overline{J}]\widetilde{\mathbf{W}} + O^2(\widetilde{\mathbf{W}}) + ... \tag{4}$$

Taking only the first order terms, the equation (4)reduces to:

$$\widetilde{\mathbf{F}} = [\overline{J}]\widetilde{\mathbf{W}} \tag{5}$$

Also note that, any perturbed flow variable in the time domain has a simple harmonic pattern with known radial frequency ω. Thus for $\widetilde{\mathbf{W}}$:

$$\widetilde{W} = \widehat{W}e^{i\omega t} = \mathcal{A}_W e^{i(\omega t + \varphi_X)} \tag{6}$$

Therefore, we can write the Linearized Harmonic equations in terms of Jacobian of the mean flow, $\overline{J}$, and the perturbation variable in frequency domain $\widehat{\mathbf{W}}$

$$i\omega\int\widehat{\mathbf{W}}d\Omega + \oint[\overline{J}]\widehat{\mathbf{W}}dA = 0 \tag{7}$$

Now, both the imaginary and the real parts of this equation should be solved. The solution is done by a pseudo-time marching method in the frequency domain.

$$\widehat{\mathbf{W}}_{new} = \widehat{\mathbf{W}}_{old} + \left(i\omega\widehat{\mathbf{W}}_{old} - \frac{\sum[\overline{J}]\widehat{\mathbf{W}}_{old}A}{\Omega}\right)\Delta\tau \tag{8}$$

The Jacobian matrix has four eigenvalues which are $\overline{\lambda}_1 = \overline{\lambda}_2 = \overline{U}_n$, $\overline{\lambda}_3 = \overline{U}_n + \overline{a}$and $\overline{\lambda}_4 = \overline{U}_n - \overline{a}$. These are the speeds by which information propagates from cell to cell in the normal direction. Flux Vector Splitting (FVS) methods permit an uneven information distribution on flux calculation by increasing the effect of the upwind side, which is needed

for hyperbolic equations such as Euler. One of the most established methods is the Steger-Warming FVS. The original form of the Steger-Warming Flux Vector Splitting method is given as follows:

$$\overline{\mathbf{F}} = \overline{\mathbf{F}}^{+} + \overline{\mathbf{F}}^{-} \tag{9}$$

$$\overline{\mathbf{F}}^{+} = [\overline{J}]^{+}\overline{\mathbf{W}}_{L} \qquad \overline{\mathbf{F}}^{-} = [\overline{J}]^{-}\overline{\mathbf{W}}_{R} \tag{10}$$

Fluxes $\overline{\mathbf{F}}^{+}$ and $\overline{\mathbf{F}}^{-}$ do not need to be changed for the Linearized Euler methodology.

$$[\overline{J}^{+}] = [\overline{T}]_{L}[\overline{\Lambda}^{+}][\overline{T}]_{L}^{-1} \qquad [\overline{J}^{-}] = [\overline{T}]_{R}[\overline{\Lambda}^{-}][\overline{T}]_{R}^{-1} \tag{11}$$

BOUNDARY CONDITIONS

Harmonic oscillating wall boundary condition

We have utilized the characteristic-based boundary conditions since our solver is FVS based. The steady boundary conditions can be found in many sources in the literature [Blazek, 2006]. The characteristics-based oscillating wall boundary condition is given in Hall's study [Hall, 1987] as:

$$\widetilde{u}\cdot\overrightarrow{n} = \frac{\partial\widetilde{r}_n}{\partial t} + u_t\frac{\partial\widetilde{r}_n}{\partial s} - \widetilde{r}\cdot\nabla(u_n) \tag{12}$$

The boundary condition given in equation (12) is adapted and implemented in our solver. Here, $\widetilde{r}$ is the oscillating position vector of the wall surface around the mean value, and s is the surface arc length. For a 3D solver second term with arc length derivative can be taken as $u_t\overrightarrow{\tau}\cdot\nabla(\widetilde{r}_n)$ where $\overrightarrow{\tau}$ is the wall unit tangent vector. If we assume that all perturbations are harmonic, the time derivative in the $\frac{\partial\widetilde{r}_n}{\partial t}$ can be replaced by $i\omega$. The term $u_t\frac{\partial\widetilde{r}_n}{\partial s}$ represents the effects due to the rotation of the aerodynamic body. Finally, the last term $\widetilde{r}\cdot\nabla(u_n)$ is to compensate for the fixed grid. It is an extrapolation from the position of the instant to its mean (steady state) location. However, it is observed that neglecting this term results in better accuracy.

$\widetilde{r}$ could occur due to rotation, translation and its combination. Since the equation is separated into real and imaginary parts, implementing a phase difference between two different motions is also possible. This condition gives us the fluctuating velocity at the surface of the airfoil. For other primitive variables, face values are taken the same as the domain. Later, primitive variables are converted to conservative ones for convenience.

Harmonic farfield boundary conditions

Harmonic far field boundary condition is derived by splitting variables in the steady far field BC into mean and the fluctuating parts. The steady far field condition used here are characteristic-based and given as follows:

Supersonic inflow:

All the information is coming from the upstream. Therefore no effects from the harmonic motion transferred to boundary condition.

$$\widetilde{p} = 0, \widetilde{T} = 0, \widetilde{u} = \overrightarrow{0} \tag{13}$$

Supersonic outflow:

All the information is coming from the upstream. Therefore, all domain perturbations directly determine boundary condition values.

$$\widetilde{p} = \widetilde{p_d}, \widetilde{T} = \widetilde{T_d}, \widetilde{u} = \widetilde{u_d} \tag{14}$$

Subsonic inflow:

Pressure information is coming from the domain and the rest is coming from the upstream.

$$\widetilde{p} = \widetilde{p_d}, \widetilde{T} = 0, \widetilde{u} = \overrightarrow{0} \tag{15}$$

Subsonic outflow:

Pressure information is coming from the downstream and the rest is coming from the domain.

$$\widetilde{p} = 0, \widetilde{T} = \widetilde{T_d}, \widetilde{u} = \widetilde{u_d} \tag{16}$$

In these equations, subscript $_d$ stands for the domain variables.

TEST CASES

Two test cases are utilized for analyzing the plunging and pitching motion of the airfoil, respectively. The test cases involve a NACA0012 airfoil with farfield boundaries. Mach number is taken as 0.1 for both cases. For the plunging motion case, the amplitude of motion is taken as 3% of the chord length, whereas the pitching motion test case has a maximum rotation angle of 5 degrees with the rotation center of 25% of the chord. The mesh for the test cases is shown in the Figure 1. Both unsteady CFD analysis with moving mesh and Linearized Euler solver uses the same grid. In the unsteady case, the grid around the airfoil is deforming by desired prescribed motion. Vibration frequency is taken as 4π rad/s as sine wave (0.5s full period), and time step for unsteady analysis taken as 1e-4. Related pressure coefficient results on the airfoil are collected from 0.25, 0.5, 0.75 times of the period and full period.

The arc in the upstream side has a radius of 10 times of the chord length (10c), and distance from trailing edge to end of the downstream is 8c.

The derived farfield equations are used for the outer boundary, and the airfoil boundary uses oscillating wall BC.

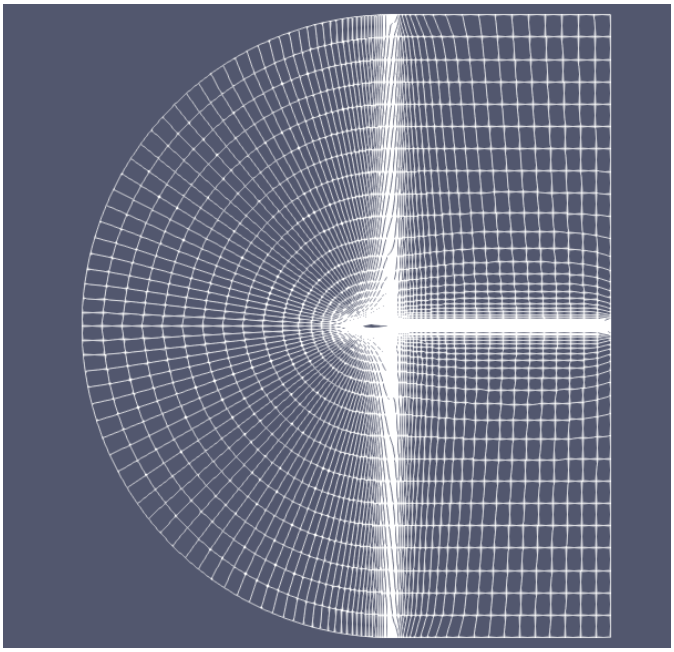

Figure 1: The mesh

RESULTS AND DISCUSSION

A mesh independence study is performed to achieve grid convergence in terms of perturbation variables. We have observed in this process that the linearized solutions are very sensitive to mesh sizes at high pressure gradient locations. The inaccuracies at the mean flow solution tend to be amplified into the perturbation solution. We have observed that, the solution accuracy requires refined cells and good orthogonality around airfoil wall to get accurate results. It is seen that the boundary conditions given at equation (12) affects at the near vicinity of the wall and a finer mesh around the moving wall is necessary.

Figure 2 demonstrates that periodicity is reached in terms of fluxes. Unsteady solutions are run for ten near-identical cycles to make sure periodicity is reached, and this fact is checked from the vertical force of the airfoil (Figure 2), although it is observed that inviscid unsteady analysis of these cases does not need more than three full cycles. However, this number could grow for viscous or turbulent cases. Even with a course mesh, only one cycle of the unsteady analysis took about 1.7 times of a complete linearized solution (without steady state part). Considering 10 periods of solution time, presented method provides 17 times faster solution speeds, and this factor will get bigger for finer grids. Thus, the time efficiency of the current methodology is unassailable.

Resulted pressure plots of the upper surface of airfoil for test case 1 and 2 could be seen below at Figures 3 and 4 respectively.

Results shows that current linearized Euler Solver can capture the general trend in terms of pressure. In general, deviations are considerably small in both cases. It should be noted that instantaneous pressure fields calculated both by unsteady CFD and harmonic method

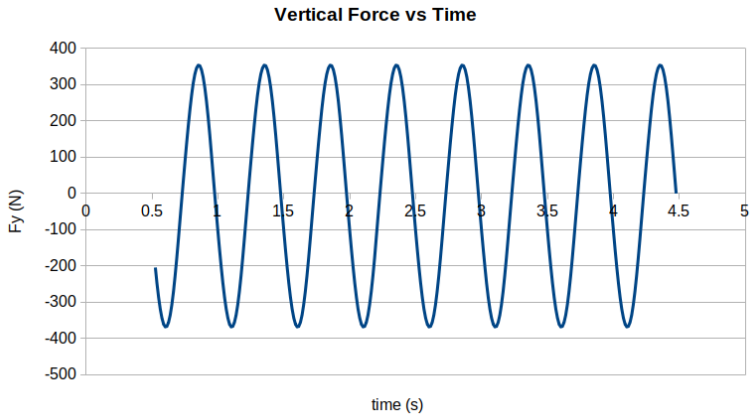

Figure 2: Vertical Force vs time

are much more aligned with each other when airfoil position is close to its equilibrium point in pitching motion test case.

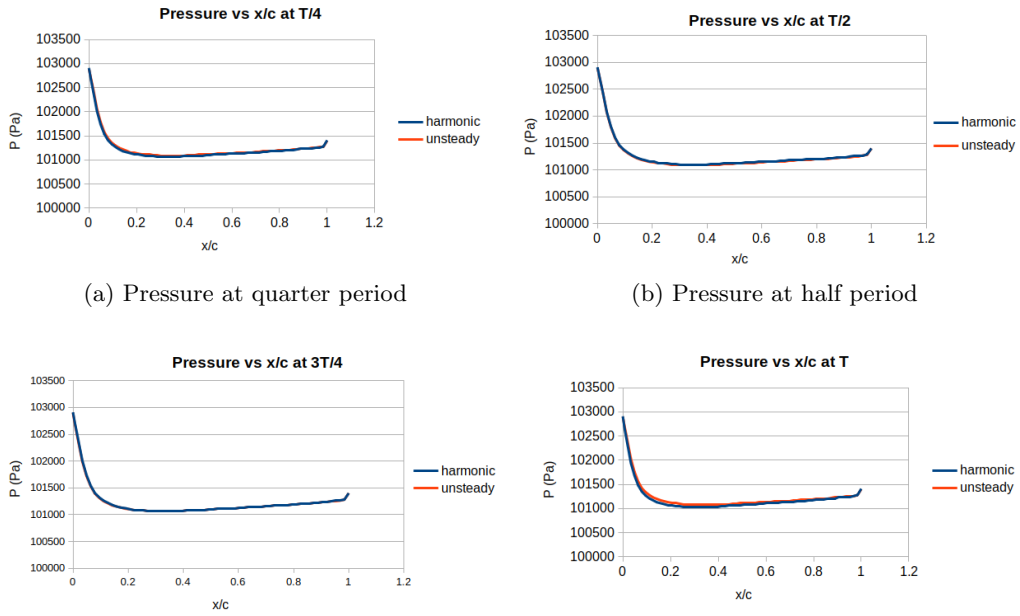

(a) Pressure at quarter period

(b) Pressure at half period

(c) Pressure at 3/4 period

(d) Pressure at full period

Figure 3: Pressure plots of the upper surface of plunging airfoil in (a,b,c,d shows sub times levels 0.25,0.5,0.75,1 times of the period respectively)

CONCLUSIONS

In this study, we have accomplished to implement FSI capabilities with prescribed perturbations to our Linearized Euler solver which is based on the Flux Vector Splitting approach. The both test results look very promising. There is no actual compromise from accuracy for the sake of solution time, and it exceeds the industry needs.

In both plunging and pitching motion cases, the Linearized Harmonic method develop in our group provide very quick and efficient solutions using much less computational resources. Our solver is very stable and the solutions are acceptable. The results are good enough to calculate lift and moment accurately for many applications. The Flutter analysis is considered as one of those applications, since the total force response is more important than the pressure distribution itself.

For future, there are many branches for improvement and further development of our solver. NS solver with turbulence modeling can be implemented to increase relevant engineering cases which the solver can handle. Secondly, non-linear harmonic methodologies can be added for more accurate solution requirements. Also, we are planning to add a structural mode shape based solver for two way coupled solutions in frequency domain.

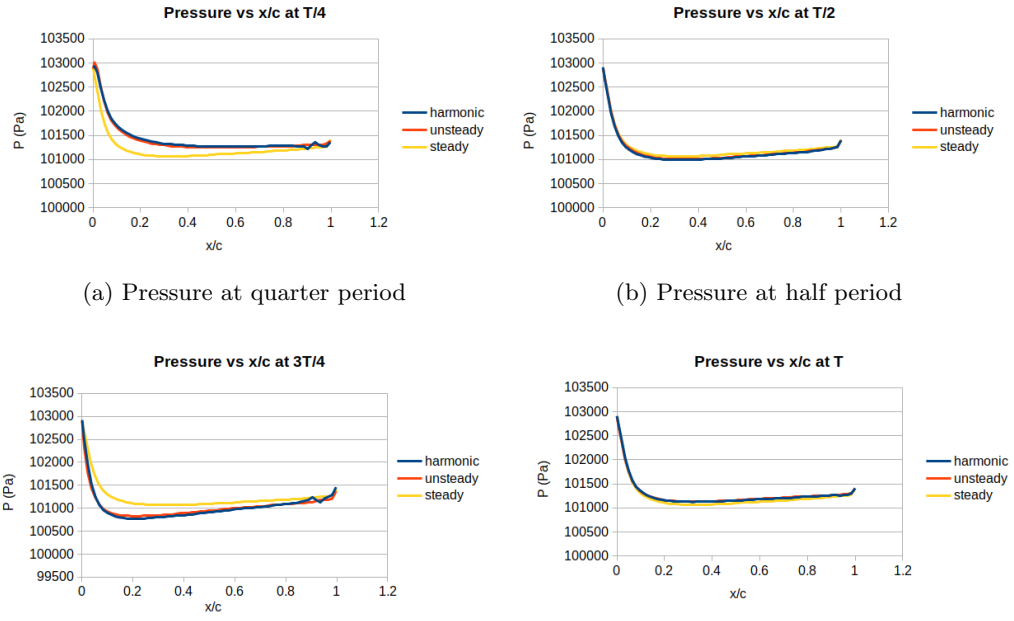

(a) Pressure at quarter period

(b) Pressure at half period

(c) Pressure at 3/4 period

(d) Pressure at full period

Figure 4: Pressure plots of the upper surface of pitching airfoil (a,b,c,d shows sub times levels 0.25,0.5,0.75,1 times of the period respectively)

References

Blazek, J. (2006). *Computational Fluid Dynamics: Principles and Applications (2nd ed.)*. Elsevier Science.

Dufour, G., Sicot, F., Puigt, G., Liauzun, C., and Dugeai, A. (2010). Contrasting the Harmonic Balance and Linearized Methods for Oscillating-Flap Simulations. *AIAA Journal*, 48(4):788–797.

Ekici, K. and Hall, K. C. (2011). Harmonic Balance Analysis of Limit Cycle Oscillations in Turbomachinery. *AIAA Journal*, 49(7):1478–1487.

Gong, Y. and Zhang, W. (2019). Efficient Aeroelastic Solution Based on Time-Spectral Fluid-Structure Interaction Method. *AIAA Journal*, 57(7):3014–3025.

Hall, K. C. (1987). *A Linearized Euler Analysis of Unsteady Flows in Turbomachinery*. PhD thesis, Massachusetts Institute of Technology.

Howison, J., Thomas, J., and Ekici, K. (2017). Aeroelastic analysis of a wind turbine blade using the harmonic balance method. *Wind Energy*, 21(4):226–241.